

Three Output Noise Generator

Micah Jeffries

California Polytechnic State University - SLO
mjjeffri@calpoly.edu

Kyle Chang

California Polytechnic State University - SLO
kchang48@calpoly.edu

Abstract - This paper documents the design process and the experimental results of an analog-based processor that outputs three different types of noise. The first noise output is a band-limited white noise which contains a flat PSD in the bandpass region. The second output is a band limited pink noise - this output contains a -10dB/dec slope in the bandpass region. The final output is a narrow-band noise with tunable central frequency using an adjustable clock signal.

I. INTRODUCTION

With many modern electronic devices operating on small power consumption, it is important to characterize the noise performances of these circuits since low-power and low-noise are conflicting requirements. Noise generators are electronic test equipment that help characterize the noise performance and other important noise parameters including the frequency response and noise figure [1]. Noise generators are often used in technical engineering fields such as telecommunications and acoustics [1].

The noise generator implemented in this project inputs the shot noise of a BJT and applies voltage amplification and frequency shaping operations to output three types of band limited noise. The three outputs of the noise generator are white noise, pink noise, and narrow-band noise with a tunable central frequency. Figure 1 shows the system level diagram for this noise generator.

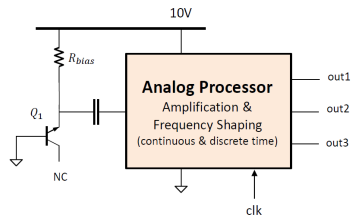


Figure 1: Noise Generator System Level Diagram [2].

This paper documents the design process and experimental results of this noise generator. The first discussion point is the characteristics of the BJT which generates the white noise. Then, each subsystem of the analog processor and their noise shaping contributions on the three outputs are discussed in their own section. Finally, MATLAB analysis on each output signal experimentally verifies the desired operation by providing three different statistical descriptions: the probability density function (PDF), the autocorrelation function (ACF), and the power spectral density (PSD).

II. BJT MODELING

The first derivation models the linear characteristics of a 2N3904 BJT. The BJT operates in reverse bias mode across the base-emitter with a $10\mu\text{A}$ bias current, and the PN junction generates white noise from avalanche breakdown. The schematic of the BJT connections, as shown in Figure 1, require a bias resistor and a coupling capacitor to generate the white noise at the input.

To determine the linear characteristics of the BJT, the circuit in Figure 2 evaluated the breakdown characteristics of the BJT. The DC supply swept from 8.5V to 10V, and five data points about the $10\mu\text{A}$ point from the I_E vs V_{EB} plot were modeled as a polynomial as shown in Figure 3.

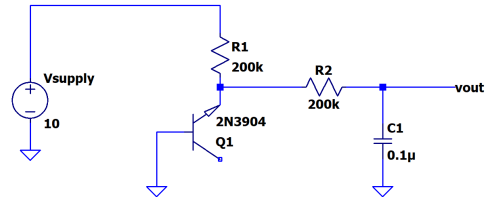


Figure 2: Base-Emitter Breakdown Test Circuit Schematic.

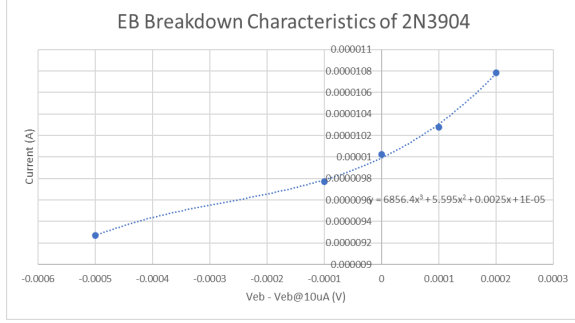


Figure 3: Reverse Breakdown Characteristics of 2N3904 BJT operating with 10uA of current.

A third order polynomial approximated the curve on the plot to extract the coefficients found in Equation (1). The equation on plot in Figure 3 provides the coefficients of this polynomial approximation.

$$I_e = 10\mu A + a_1\Delta v + a_2\Delta v^2 + a_3\Delta v^3 \quad (1)$$

$$I_e = 10\mu A + 0.025\Delta v + 5.595\Delta v^2 + 6856.4\Delta v^3$$

where $\Delta v = V_{EB} - V_{EB@10\mu A}$

The extracted polynomial approximation of the BJT in breakdown mode simplifies into a linear model of the BJT. Equations (2-4) represent the values of the linear model.

$$R_{Th} = 1/a_1 = 500 \Omega \quad (2)$$

$$V_{Th} = V_{EB@10\mu A} = 7.769 V \quad (3)$$

$$NSD = 2\sqrt{(kT \cdot R_{Th})} = 2.53 \text{ nV}/\sqrt{\text{Hz}} \quad (4)$$

III. ANALOG PROCESSOR

The architecture of the analog processor contains three main circuits: the Butterworth low-pass filter, the pink noise filter, and the switch-capacitor bandpass filter. Figure 4 presents all three subsystems as black box diagrams. The following sections document the theory and design for each subcircuit.

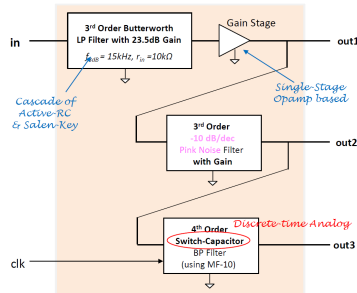


Figure 4: Three Main Subsystems of the Noise Generator [2].

The first subcircuit is the 3rd order Butterworth low pass filter. This circuit limits the upper frequency band to 15 kHz for all three outputs. The filter design is a cascade of a 2nd order Sallen-Key filter and an active RC filter to produce a 3rd order filter. The design requirements for this filter are a -3dB cutoff frequency at 15 kHz, a total gain of 23.5 dB, and an input resistance of 10kΩ [2].

The second subcircuit is the pink noise filter. The design of this circuit involves the bridging of multiple resistor and capacitor pairs across the negative feedback of an op amp to produce the characteristic -10dB/decade slope of the filter. This design is based on an active filter proposed by A.L. Dalcastagne and S. N. Filho [4].

The final subsystem is a switch capacitor bandpass filter. This subsystem used of the MF10 IC designed by Texas Instruments to produce a narrow band noise signal. This device consists of two independent CMOS 2nd order active filters and when configured with external resistors and a clock signal, the cascaded system yields a 4th order bandpass filter with adjustable center frequency [2].

IV. BUTTERWORTH LP FILTER

The first element of the analog processor is the 3rd order Butterworth filter. The design of this filter consists of a cascade of a 1st order active low-pass filter and a 2nd order Sallen-Key low-pass filter. Figure 5 shows the schematic for this cascaded filter. The schematic also includes the linear model of the BJT input as derived in the BJT modeling section.

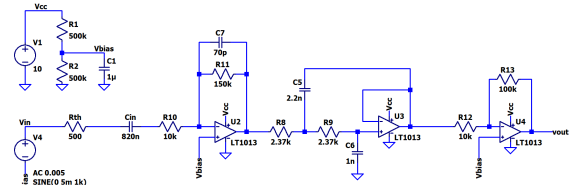


Figure 5: Schematic of 3rd order Butterworth Low Pass Filter.

The design of the 1st order active low pass filter provides the topology necessary to meet the gain specification by applying the appropriate ratio of input resistance to feedback resistance. The op-amp is

then designed as a low pass filter by bypassing a capacitor across the feedback resistance (see Appendix for derivations). In addition, the circuit added a unity gain buffer stage at the output for any gain compensation required after validation.

The 2nd order Sallen-Key low pass filter provided unity passband gain and a 15kHz cutoff frequency to increase the overall system order. Equation (5) presents the design equations to calculate the cutoff frequency from the resistor and capacitor values [5]. The resistor values are set equal in value to simplify calculations. The only other constraint was that the ratio of the capacitor values meet the condition shown in Equation 6.

$$f_0 = 1/\sqrt{(R_1 R_2 C_1 C_2)} \quad (5)$$

$$C_1/C_2 > 4Q^2 \quad (6)$$

$$\text{where } Q = \sqrt{(R_1 R_2) / (R_1 + R_2)} * \sqrt{(C_1/C_2)} \quad (7)$$

An additional desired specification is that the amplifiers operate on a single supply voltage of 10 V. Thus, an additional biasing circuit provided a mid-supply DC bias at 5V to the noninverting inputs of the op-amps.

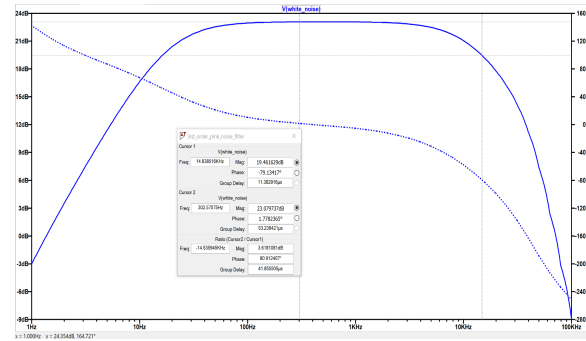


Figure 6: Simulation of 3rd Order Butterworth Filter Producing Band-Limited White Noise.

As seen in Figure 6, the schematic meets the desired gain specification of 23.5 dB in the passband with an upper cutoff frequency at 15kHz. The simulation results at higher frequencies also display the characteristic -60 dB/decade slope of a 3rd order filter. The high-pass filter response in the lower frequency range is due to the AC coupling capacitor at the BJT emitter terminal.

V. PINK NOISE FILTER

The next component in the analog processor is the pink noise filter responsible for the characteristic -10dB/decade slope within the same passband of the white noise generated from the Butterworth filter. Figure 7 shows the schematic for the pink noise filter.

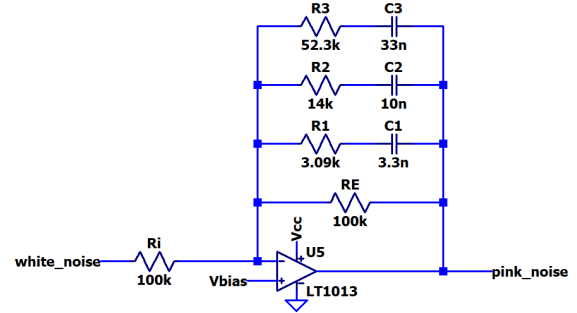


Figure 7: Pink Noise Filter Schematic [3].

Table 1: Normalized Pink Noise Filter Resistor and Capacitor Values [3].

n	8	7	6	5	4	3	2
$R_1 (\Omega)$	1.532	1.428	1.084	8.572×10^{-1}	7.385×10^{-1}	5.286×10^{-1}	2.770×10^{-1}
$C_1 (F)$	1.769×10^{-3}	1.080×10^{-3}	1.155×10^{-3}	9.108×10^{-3}	4.804×10^{-3}	3.087×10^{-3}	2.089×10^{-3}
$R_2 (\Omega)$	6.435×10^{-1}	5.865×10^{-1}	4.046×10^{-1}	2.913×10^{-1}	2.344×10^{-1}	1.404×10^{-1}	4.276×10^{-2}
$C_2 (F)$	9.983×10^{-3}	5.890×10^{-3}	5.450×10^{-3}	3.764×10^{-3}	1.822×10^{-3}	9.611×10^{-4}	4.835×10^{-4}
$R_3 (\Omega)$	3.039×10^{-1}	2.698×10^{-1}	1.665×10^{-1}	1.073×10^{-1}	7.834×10^{-2}	3.120×10^{-2}	—
$C_3 (F)$	5.008×10^{-3}	2.866×10^{-3}	2.533×10^{-3}	1.435×10^{-3}	6.564×10^{-4}	3.576×10^{-4}	—
$R_4 (\Omega)$	1.468×10^{-1}	1.265×10^{-1}	6.912×10^{-2}	3.880×10^{-2}	2.015×10^{-2}	—	—
$C_4 (F)$	2.457×10^{-3}	1.367×10^{-3}	9.897×10^{-4}	5.576×10^{-4}	3.071×10^{-4}	—	—
$R_5 (\Omega)$	7.110×10^{-2}	5.903×10^{-2}	2.770×10^{-2}	1.057×10^{-2}	—	—	—
$C_5 (F)$	1.201×10^{-3}	6.561×10^{-4}	4.348×10^{-4}	2.873×10^{-4}	—	—	—
$R_6 (\Omega)$	3.410×10^{-2}	2.628×10^{-2}	8.190×10^{-3}	—	—	—	—
$C_6 (F)$	5.937×10^{-4}	3.299×10^{-4}	2.591×10^{-4}	—	—	—	—
$R_7 (\Omega)$	1.555×10^{-2}	8.439×10^{-3}	—	—	—	—	—
$C_7 (F)$	3.083×10^{-4}	2.299×10^{-4}	—	—	—	—	—
$R_8 (\Omega)$	5.093×10^{-3}	—	—	—	—	—	—
$C_8 (F)$	2.231×10^{-4}	—	—	—	—	—	—

The paper by A.L. Dalcastagne and S. N. Filho [4] provided the schematic and normalized resistor and capacitor values for this pink noise filter. R_1 and R_E (100k Ω resistors) in Figure 7 do not contribute to the white noise, therefore, this table is only relevant for calculating the resistor and capacitor pair values above the feedback resistance. The specifications for this filter are a 3rd order filter, which means that the relevant values lie in the column where $n = 3$ as highlighted in Table 1.

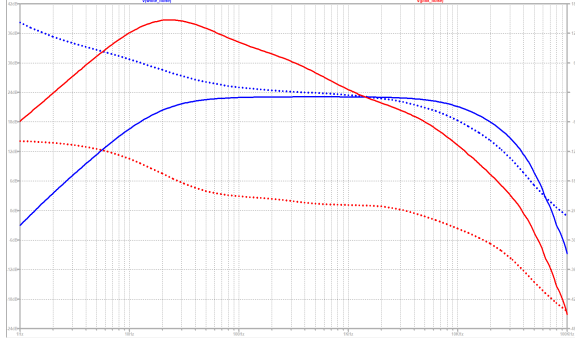


Figure 8: Simulation of Pink Noise Filter Shown (red) and White Noise Filter (blue).

The simulation result in Figure 8 shows that this filter produces the characteristic -10dB/decade slope in the passband between 25Hz and 15kHz. The steep slope at higher frequencies is due to the combined stop-band roll-off from the Butterworth filter in cascade with the pink noise filter.

VI. SWITCH CAPACITOR BP FILTER

The final component in the analog processor is the MF-10 IC designed by Texas Instruments - this device produced an adjustable narrow-band (high Q) signal. This IC produces various 2nd order filters depending on resistor configurations. For the purposes of the analog processor, the MF-10 resistors are configured for a bandpass filter which has a tunable central frequency controlled by an input clock signal.

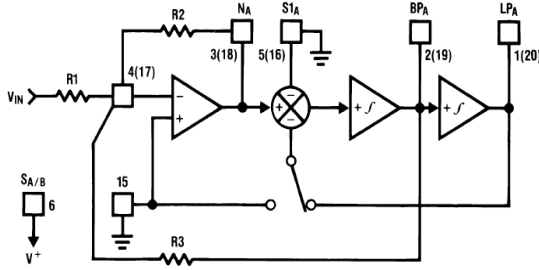


Figure 9: Schematic Configuration of MF-10 Mode 1 of Operation with Lowpass and Bandpass Outputs.

For simplicity of operation, the MF-10 operates under mode 1 (Figure 9) in the bandpass configuration. The MF-10 datasheet [2] further details the design equations.

$$H_{O_{BP}} = -R_3 / R_1 = 1 \quad (8)$$

$$Q = R_3 / R_2 = 10 \quad (9)$$

$$f_0 = f_{CLK} / 100 \quad (10)$$

$H_{O_{BP}}$ is the passband gain, Q is the quality factor, and f_0 is the center frequency. The datasheet specified a maximum value of $f_0 * Q$ to be less than 200kHz. With a maximum center frequency at 15kHz, the calculated maximum Q value is 13.33 - therefore, the selected maximum Q is 12. Since there is a cascade of two filters, the first filter's Q is 10 and the second filter's Q is 12. Figure 10 shows the schematic of the 4th order bandpass filter (see Appendix for derivations and further details).

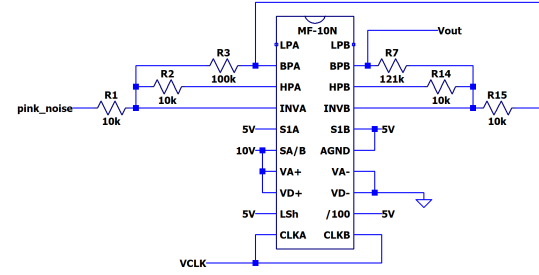


Figure 10: 4th Order BPF Schematic.

VII. WHITE NOISE

With the preliminary design work and simulation completed, system integration started with block-by-block validation - each block is divided as shown in Figure 11. The step response and frequency response for each filter confirmed desired operation (see Appendix for circuit validation). To verify correct noise generation, each output is experimentally verified by providing three different statistical descriptions: the PDF, the PSD, and the ACF.

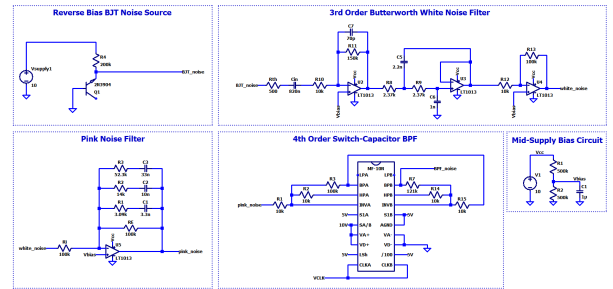


Figure 11: Analog Processor Schematic.

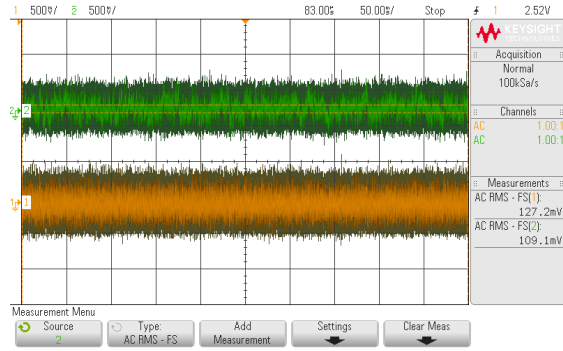


Figure 12: White Noise (Orange Signal) and Pink Noise (Green Signal) Oscilloscope Capture.

Figure 12 shows an oscilloscope capture of the white noise (orange) and the pink noise together (green). The white noise appears evenly distributed, indicating that the signal contains equal frequency content within the 15 kHz passband. The output RMS voltage is $127.2\text{mV}_{\text{RMS}}$ which exceeds the $100\text{mV}_{\text{RMS}}$ specification required to supply the following pink noise filter.

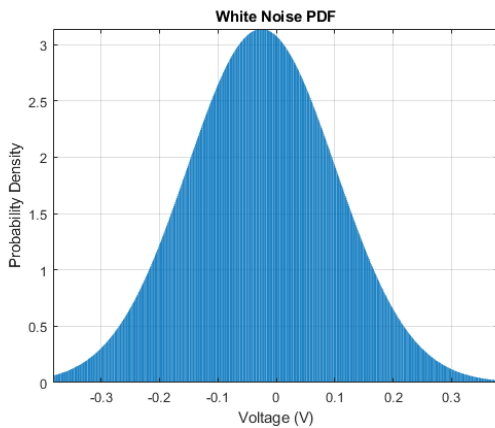


Figure 13: Post-Processed MATLAB PDF of White Noise Output Signal.

Figure 13 shows the normal distribution PDF plot of the post-processed white noise signal in Figure 11. As expected of a Gaussian white noise signal, the average voltage is approximately 0 V. The standard deviation, which defines the range of the signal amplitude, is approximately 143.2 mV. This is justified by the RMS value of the white noise at approximately $127.2\text{mV}_{\text{RMS}}$, as shown in Figure 11, since the RMS and standard deviation are the same value theoretically.

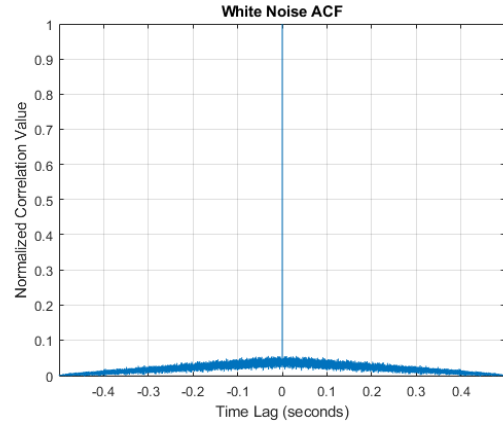


Figure 14: Post-Processed MATLAB ACF of White Noise Output Signal.

The ACF of the white noise signal is shown in Figure 14. In a pure white noise signal, the ACF is simply an impulse at a lag time of 0 seconds. The ACF of Figure 14 shows an impulse at zero, however, in a band-limited white noise signal, the ACF will contain small, non-zero correlation values that gradually decrease as the lag time approaches the duration of the sampled signal (0.5 seconds).

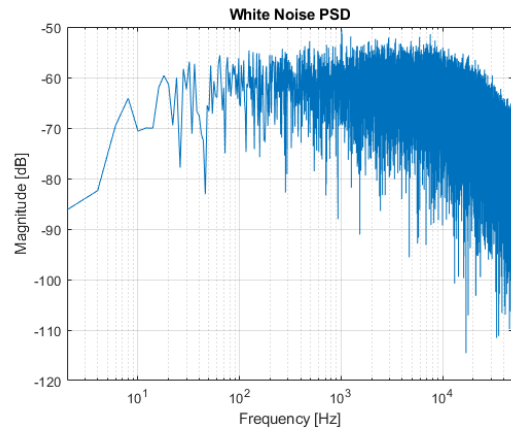


Figure 15: Post-Processed MATLAB PSD of White Noise Output Signal.

The PSD of the white noise signal is shown in Figure 15. The PSD has a flat passband region and, once it reaches the 15kHz cutoff frequency, there is a -60dB/decade descent as expected in a 3rd order filter. Between DC and 25Hz, the frequency response slopes at +20dB/decade - this is from the 1st order high pass filter. Thus, the PSD confirms the expected output of a band limited white noise signal with a cutoff frequency specified by the 3rd order Butterworth low pass filter and input AC coupling.

VIII. PINK NOISE

The second block constructed and analyzed is the pink noise filter. The oscilloscope capture in Figure 11 displays the pink noise output as the green signal. The pink noise is considerably more ‘choppy’ than the white noise signal. This is expected since the passband region for pink noise is now more heavily influenced by its lower frequency content due to the -10dB/dec low-pass filter - the result is unequal frequency distribution.

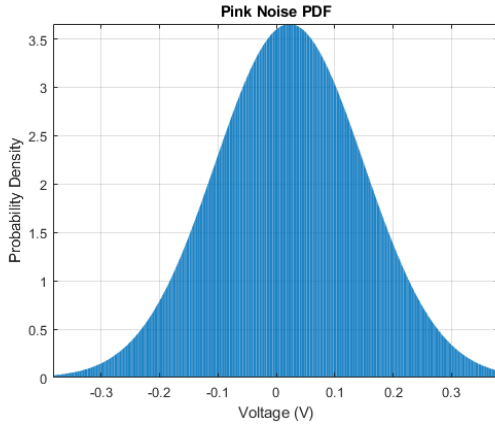


Figure 16: Post-Processed MATLAB PDF of Pink Noise Output Signal.

Figure 16 shows the Gaussian distribution PDF of the post-processed pink noise signal from Figure 9. As expected of a random process type signal, the average sample value is approximately 0 V. The standard deviation is 126.5 mV - this is close to the 109.1 mV_{RMS} measurement shown in Figure 9.

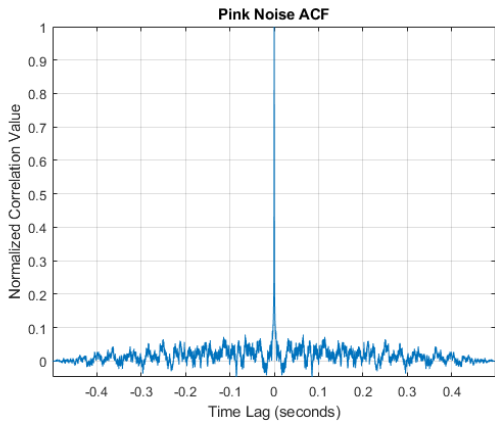


Figure 17: Post-Processed MATLAB ACF of Pink Noise Output Signal.

Figure 17 shows the ACF of the pink noise signal. This ACF has a correlation peak at 0 seconds and a gradual decay in amplitude due to limited sample size similarly seen in the white noise ACF. In addition, the ACF shows some form of periodicity. This indicates a narrower range of frequency content in pink noise which results in greater correlation in the output signal.

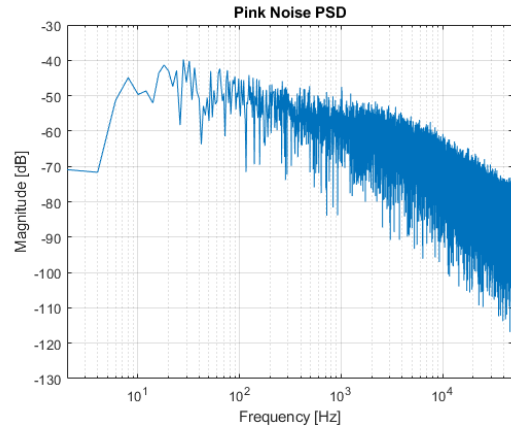


Figure 18: Post-Processed MATLAB PSD of Pink Noise Output Signal.

Figure 18 shows the PSD of the pink noise signal. Because of the low-pass nature of the pink filter, frequency content in the passband is attenuated at -10dB/decade between 25Hz and 15kHz. The PSD begins a -70dB/decade descent once it reaches the 15kHz cutoff frequency due to the cascaded -60dB/decade from the white noise filter.

IX. NARROW-BAND NOISE

The narrow-band noise output generated by the switched-capacitor bandpass circuit is the final subsystem analyzed. Figure 19 shows the oscilloscope capture of the bandlimited signal output and the corresponding input clock signal at 500kHz. According to calculations and measurements, the output 5kHz frequency is 100 times less than 500kHz input clock signal frequency (see Appendix). The 5kHz frequency content dominated the output signal. There is observable noise in the signal originating from the pink noise output.

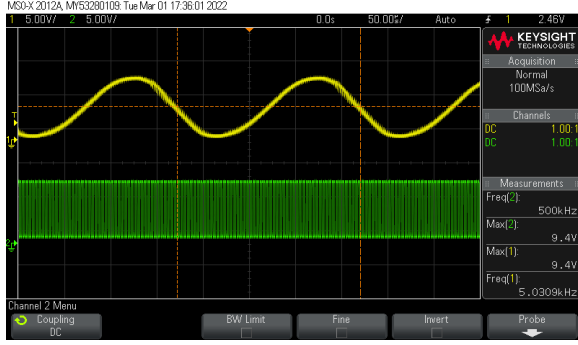


Figure 19: Oscilloscope Capture of Bandlimited Noise Signal (Yellow) and Clock Signal (Green).

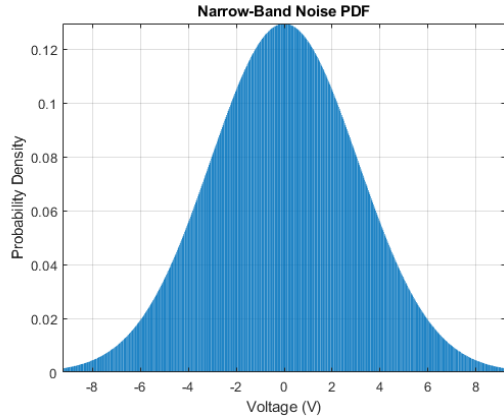


Figure 20: Post-Processed MATLAB PDF of Narrow-Band Noise Output Signal.

Figure 20 shows the Gaussian distribution PDF plot of the post-processed narrow-band noise signal in Figure 19. The average sample value is approximately 0V and the standard deviation is approximately 3V. The standard deviation is approximately the RMS of the output signal at $\sim 3.3V$.

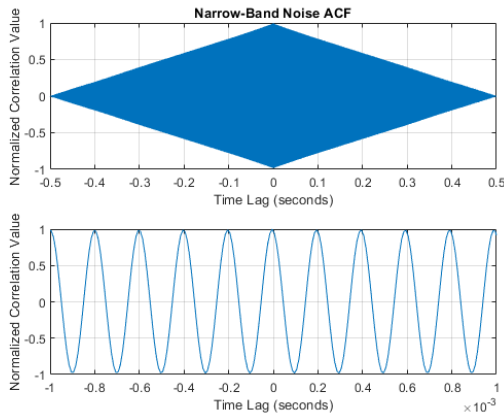


Figure 21: Post-Processed MATLAB ACF of Narrow-Band Noise Output Signal.

The ACF of the narrow-band noise signal is shown in Figure 21. Since the 5kHz output dominated the signal, the ACF displayed sinusoidal variations in correlation magnitude at intervals equal to the input signal's period - the frequency of autocorrelation peaks is 5kHz. Compared to white noise and pink noise ACFs, the narrow-band noise is highly correlated. The magnitude also decreases as the lag value increases due to the limited sample size.

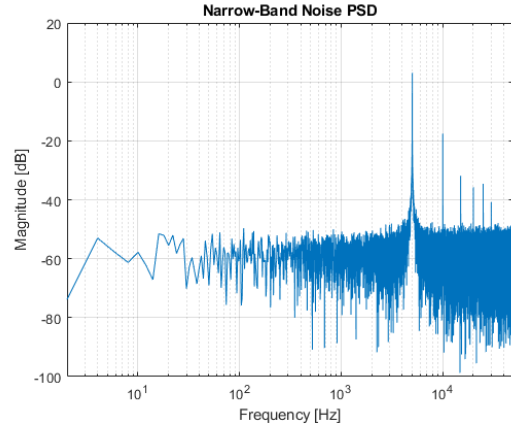


Figure 22: Post-Processed MATLAB PSD of Narrow-Band Noise Output Signal.

Figure 22 shows the PSD of the narrow-band noise signal with a peak at 5.03 kHz - this is on par with the calculated 5kHz center frequency. The PSD also displays a high $Q \approx 150$ from the 4th order cascade and over 40dBc SNR of nearby frequencies. The PSD also shows integer harmonics of 5kHz which is a result of high gain causing signal clipping as seen in Figure 19.

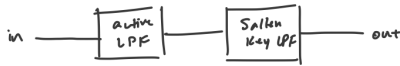
X. CONCLUSION

The analog processor designed and implemented in this paper successfully demonstrated the desired output noise spectra: a band-limited white noise signal, a pink noise signal, and a narrow-band signal. The design and validation encompassed block-by-block integration and testing to confirm desired parameters such as -3dB bandwidth, quality factor, and filter step response. Stochastic analysis (PDF, ACF, and PSD) using MATLAB confirmed the three output sources produced a 25Hz-15kHz bandwidth white noise, a -10dB/decade pink noise filter, and a narrow-band tunable noise filter.

XI. APPENDIX

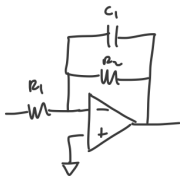
The 3rd order Butterworth LPF derivations is as follows:

3rd order LPF



- 23.5dB gain
- $f_c = 15 \text{ kHz}$
- $V_{in} = 10 \text{ k}\Omega$

Inverting 1st Order LPF

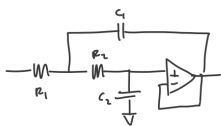


$$f_c = \frac{1}{2\pi R_2 C_1} \quad K = -\frac{R_2}{R_1} = 23.5 \text{ dB} = 14.96$$

$$R_1 = V_{in} = 10 \text{ k}\Omega \Rightarrow R_2 = 130 \text{ k}\Omega$$

$$\Rightarrow C_1 = 66 \text{ pF}$$

2nd Order Sallen-Key LPF



$$Q = 0.7071$$

$$FSF = 1$$

$$f_c = 15 \text{ kHz}$$

$$K = 1$$

$$FSF \cdot f_c = \frac{1}{2\pi \sqrt{R_1 R_2 C_1 C_2}} \Rightarrow \sqrt{R_1 R_2} =$$

$$Q = \frac{\sqrt{R_1 R_2 C_1 C_2}}{R_1 C_1 + R_2 C_2} = \frac{\sqrt{R_1 R_2}}{R_1 + R_2} \sqrt{\frac{C_1}{C_2}} \Rightarrow R_1 + R_2 = 4745 \text{ }\Omega$$

$$\frac{C_1}{C_2} \geq 4Q^2 = 2 \Rightarrow R_1 = R_2 = 2372.5 \text{ }\Omega$$

$$C_2 \geq 2C_1$$

$$C_2 = 1 \text{ nF}$$

$$C_1 = 0.5 \text{ nF}$$

The resistor values are 1% tolerance and capacitor values are 5% tolerance. The op-amps used are LMC6484 which come in quad-pack ICs. This was chosen since the specifications required high filter orders implying multiple op-amps required - using a quad-pack decreases the system's overall footprint.

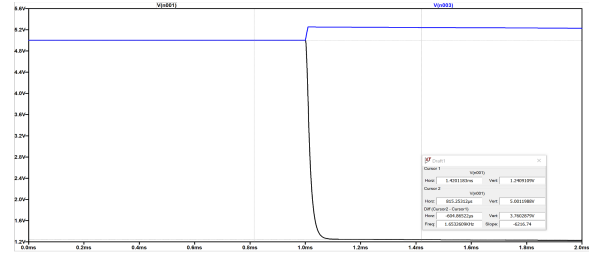


Figure 23: Simulated Step Response of 1st Order Inverting Amp.

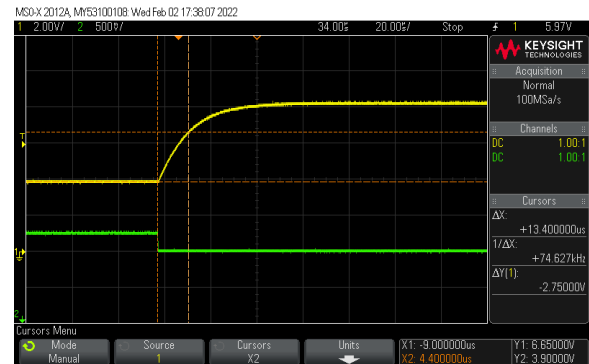


Figure 23: Measured Step Response of 1st Order Inverting Amp.

The calculated RC time constant is $\sim 10.5 \mu\text{sec}$ while the measured time constant is $13.4 \mu\text{sec}$. This confirms the amplifier is operating as expected - the error is attributed to component value tolerances.

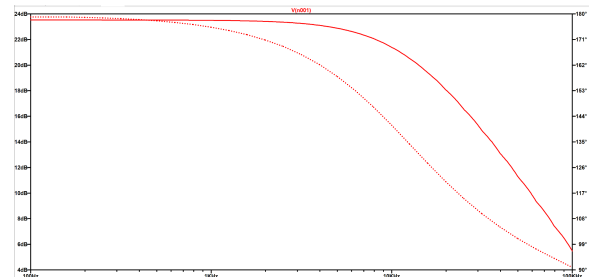


Figure 24: Simulated 1st Order Inverting Amp Frequency Response..

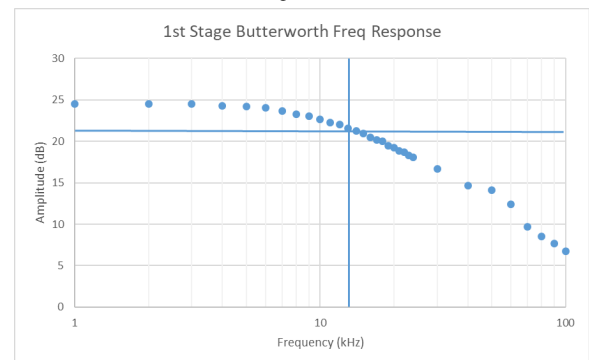


Figure 25: Measured 1st Order Inverting Amp Frequency Response.

The measured -3dB cutoff of the 1st order filter is ~13kHz which is a little lower than the simulated 15kHz. This error is attributed to not having enough frequency resolution therefore there is not enough data to pinpoint the exact cutoff frequency. However, the desired passband gain meets the simulation result at 23.5dB.

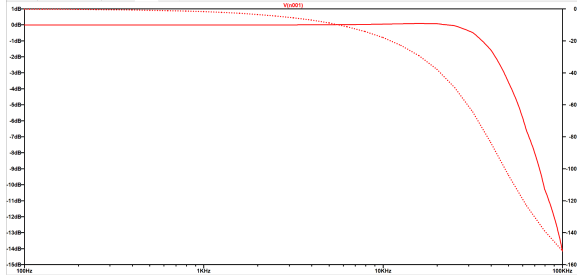


Figure 26: Simulated 2nd Order S-K Frequency Response.

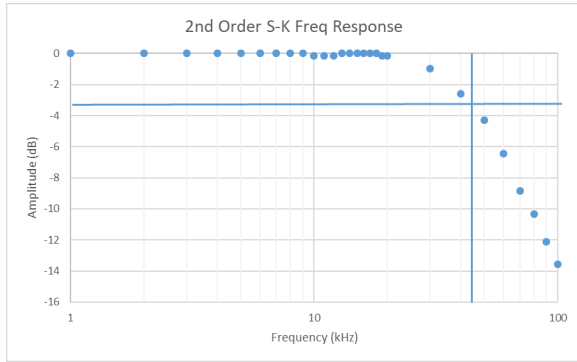


Figure 27: Measured 2nd Order S-K Frequency Response.

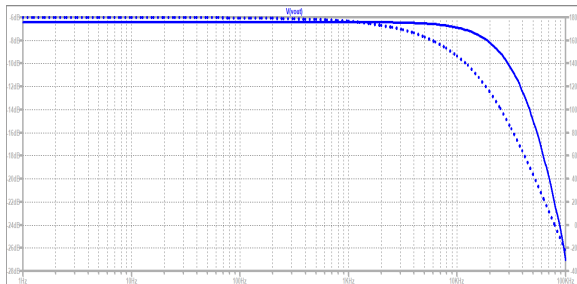


Figure 28: Simulated 3rd Order Butterworth Frequency Response.

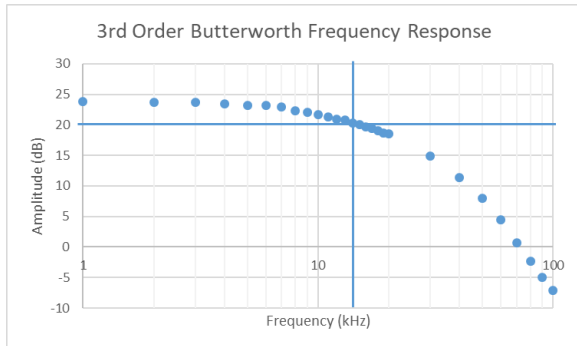


Figure 29: Measured 3rd Order Butterworth Frequency Response.

Figures 26-29 are the simulated and measured frequency responses for the 2nd order S-K filter and the complete 3rd order Butterworth filter. In the S-K filter, the measured -3dB bandwidth is ~45kHz which is slightly lower than the simulated 50kHz bandwidth. Both simulation and measurements show a unity passband gain with a very slight dip in the middle of the passband. When the S-K is cascaded after the inverting amp, the measured and simulated plots in Figure 28 and 29 yield a -3dB bandwidth at 15kHz and a passband gain at 23.5dB.



Figure 30: Measured 3rd Order Butterworth Input Noise (green), Output Noise (yellow), and FFT (pink).

Figure 30 shows the measurements captured by the oscilloscope when the BJT noise is configured as the input.

The pink noise filter topology comes from Figure 7 and the normalized resistor and capacitor values are from Table 1. These parameters from [4] calculated the designed filter as follows:

$$\text{Let } R_E = 100k\Omega$$

3rd order		
5.286×10^{-1}	→	52.86 kΩ ~ 52.3 kΩ
3.087×10^{-3}	→	30.87 nF ~ 30 nF - 30.9 nF - 31.4 nF
1.404×10^{-1}	→	14.04 kΩ ~ 14 kΩ
9.611×10^{-4}	→	9.611 nF ~ 9.53 nF - 10 nF
3.120×10^{-2}	→	3.12 kΩ ~ 3.09 kΩ
3.576×10^{-4}	→	3.576 nF ~ 3.6 nF - 3.65 nF

$$\text{E12 caps: } 3.3\mu\text{F}, 10\mu\text{F}, 33\mu\text{F}$$

Where resistor values are 1% tolerance and capacitor values are 5% tolerance. Figures 31 and 32 show the simulated and measured step response of the filter.

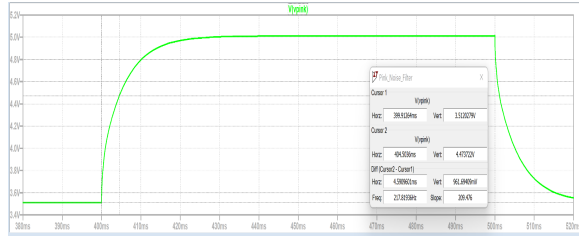


Figure 31: Simulated Pink Noise Filter Step Response.

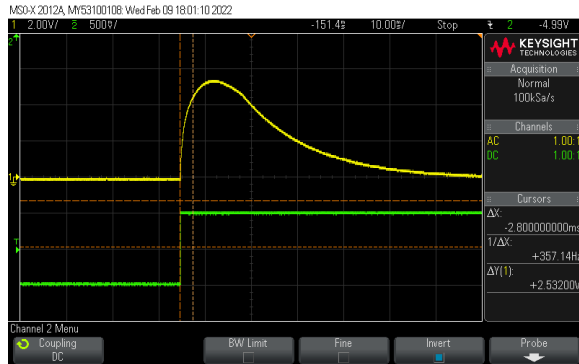


Figure 32: Measured Pink Noise Filter Step Response.

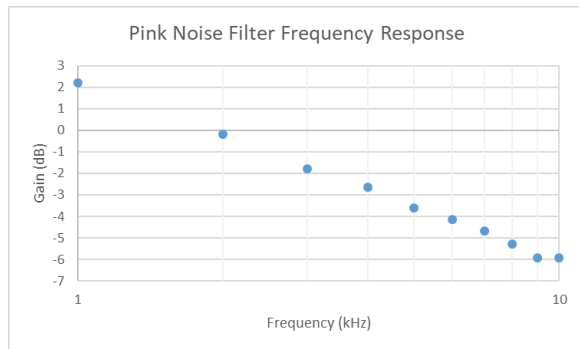


Figure 33: Measured Pink Noise Filter Frequency Response.

The measured frequency response of the pink noise filter only covers 1kHz to 10kHz, however there is $\sim 8\text{dB/dec}$ slope which is close to the desired -10dB/dec slope.

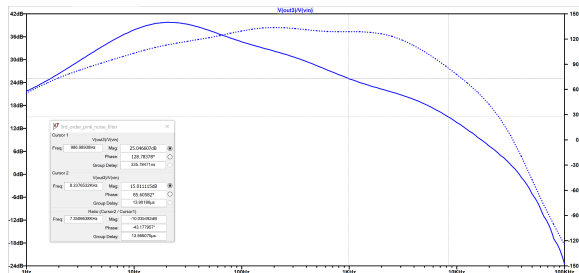


Figure 34: Simulated Pink Noise Filter Frequency Response.

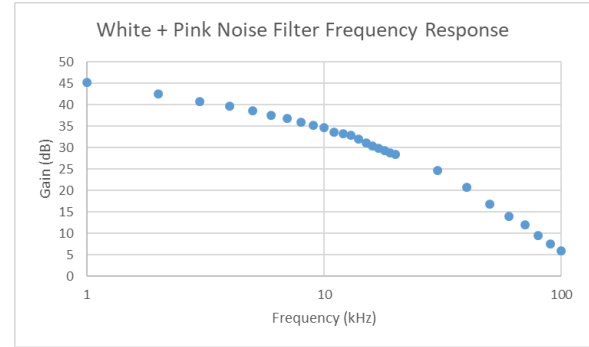


Figure 35: Measured Cascaded White & Pink Noise Filter Frequency Response.

The cascaded white and pink noise filter show the -10dB/dec slope from 1kHz to 10kHz, and a steep rolloff after 15kHz due to the attenuation from the white and pink noise filter low-pass filter response.

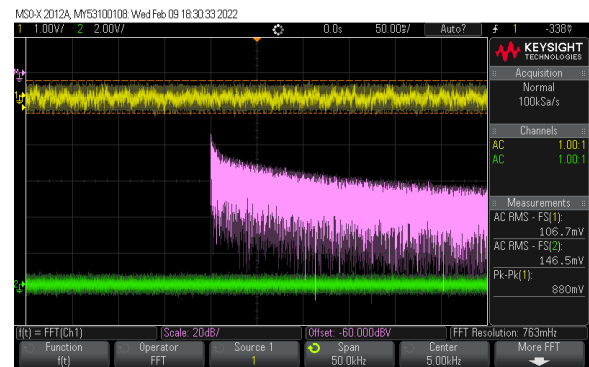


Figure 36: Measured Output Noise (green), Output Pink Noise (yellow), and Pink Noise FFT (pink).

The MF-10N resistor value calculations are based on [3] and follow the $f_0 \cdot Q$ limitation specified in the datasheet. First, the maximum Q was calculated to be 13.3, therefore the selected maximum $Q = 12$ to avoid reaching the max value. $R1$ and $R2$ were selected first at $10\text{k}\Omega$ as relatively high impedance for low power draw and since these were component values already in use. $R3$ is then calculated from $Q = R3/R2$ design equation.

$$f_0 = \frac{f_{clk}}{100} \text{ or } \frac{f_{clk}}{50}$$

$$f_2 = 20\text{kHz} - 15\text{kHz}$$

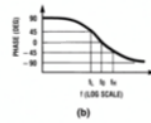
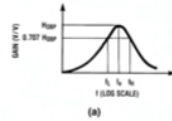
$\swarrow \quad \searrow$
 $1\text{kHz} \quad 2\text{kHz}$

$\swarrow \quad \searrow$
 $750\text{kHz} \quad 1.5\text{MHz}$

$\therefore \frac{\text{follu}}{100}$ not viable

$$\frac{f_{clk}}{50} \text{ var } 1 \text{ kHz} - 750 \text{ kHz}$$

to synthesize 20 Hz - 15 kHz



$$H_{BP}(s) = \frac{H_{OHP} \frac{\omega_O}{Q} s}{s^2 + \frac{\omega_O}{Q} s + \omega_O^2}$$

$$t_0 = \frac{t_0}{t_0 - 1}; \quad t_0 = \sqrt{t_0}$$

$$t_4 = t_0 \left(\frac{1}{20} + \sqrt{\left(\frac{1}{20} \right)^2 + 1} \right)$$

$$\omega_0 = 2\pi f_0$$

Figure 17. 2nd-Order Bandpass Response

→ Div by 100 is better apparently,
and we can drive high freq

$f_{\text{notch}} = f_0$ (See Figure 23)

$$= \frac{f_{\text{CLK}}}{100} \text{ or } \frac{f_{\text{CLK}}}{50}$$
$$H_{OLP} = \text{Lowpass gain (as } f \rightarrow 0) = -\frac{R_2}{R_1}$$

$$H_{OLP} = \text{Lowpass gain (as } f \rightarrow 0) = -\frac{R_2}{R_1}$$

$$H_{OBP} = \text{Bandpass gain (at } f = f_0) = -\frac{R_3}{R_1}$$

$$H_{ON} = \text{Notch output gain as } \left. \begin{array}{l} f \rightarrow 0 \\ f \rightarrow f_{CLK}/2 \end{array} \right\} = \frac{-R_2}{R_1}$$

$$Q = \frac{f_o}{BW} = \frac{R_3}{R_2}$$

= quality factor of the complex pole pair

BW = the -3 dB bandwidth of the bandpass output.

Circuit dynamics:

$$H_{OLP} = \frac{H_{OBP}}{Q} \text{ or } H_{OBP} = H_{OLP} \times Q$$

$$= H_{ON} \times Q.$$

$$H_{OLP(\text{peak})} \cong Q \times H_{OLP} \text{ (for high } Q\text{'s)}$$

- * limitations :

$$f_0 \times Q < 200 \text{ kHz} \text{ for } f_0 > 5 \text{ kHz}$$

$$\Rightarrow \frac{200 \text{ kHz}}{15 \text{ kHz}} = 13.3 > Q$$

choose $Q=10$ for stage 1

$Q = 12$ for stage 2

stage 1 : $Q = \frac{P_2}{P_1}$

let $R_2 = 10 \text{ k}\Omega$

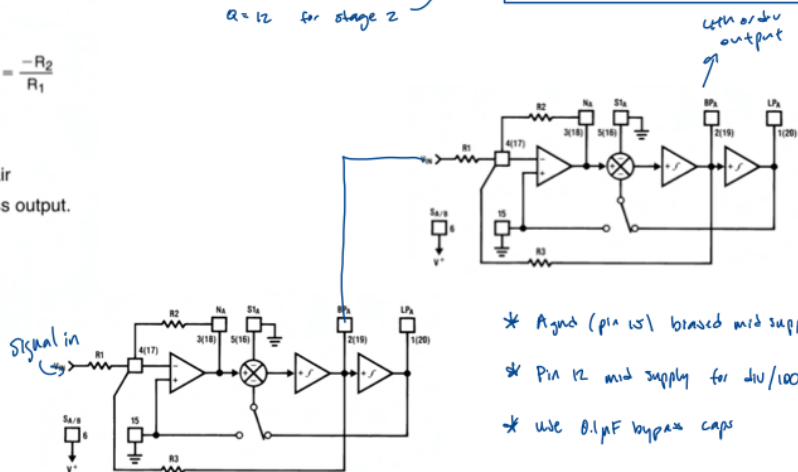
$$\Rightarrow R_3 = 100 \text{ k}\Omega$$

Stage 2: let $R_2 = 10 \text{ k}\Omega$

$$R_3 = 121 \text{ k}\Omega$$

choose $R_1 = 10k\Omega$

for unity gain



* Agnd (pin 15) biased mid supply

* Pin 12 mid supply for div/100

* use $0.1 \mu F$ bypass caps

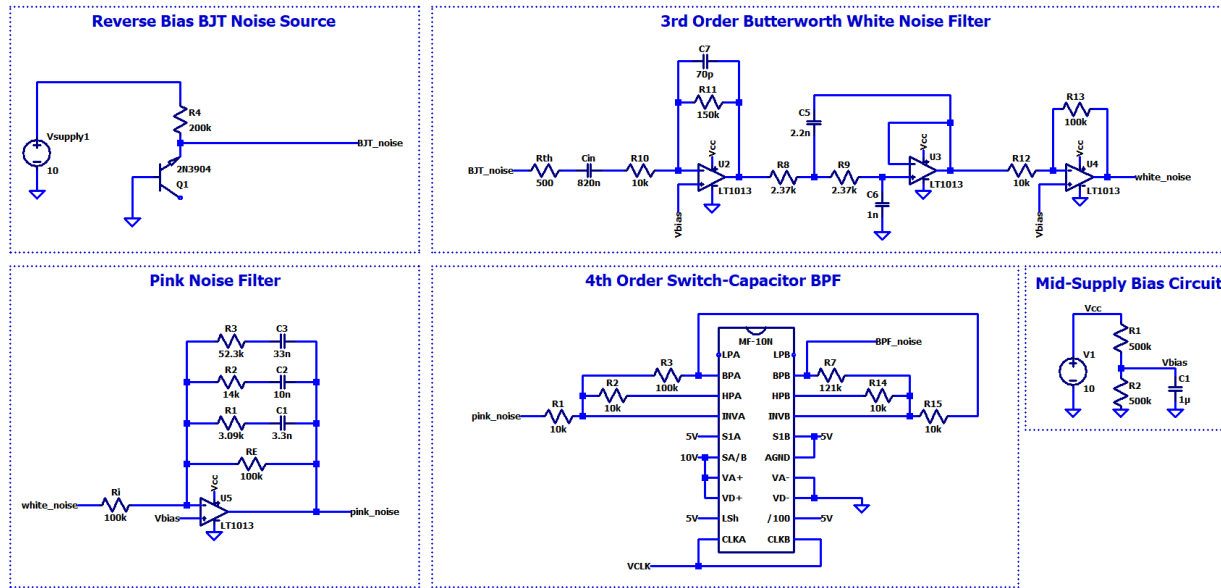


Figure 37: Analog Processor Schematics.

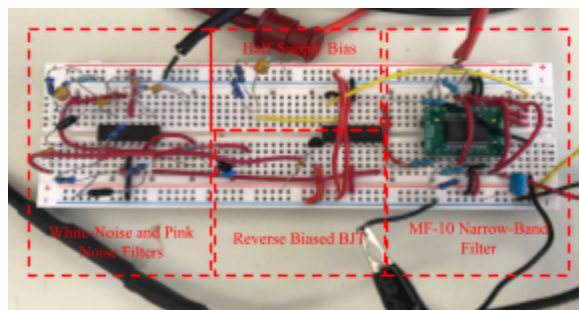


Figure 38: Analog Processor Implemented on Breadboard.

- [4] A. L. Dalcastagne and S. N. Filho, "On the Analog Generation of Pink Noise from White Noise," 2005 IEEE International Symposium on Circuits and Systems, Kobe, Japan, July 2015, pp. 1945-1947. Thus, the PSD confirms the expected output of a band limited pink noise signal.
- [5] Electronics Tutorials, "Sallen-Key Filter", electronics-tutorials.ws.

REFERENCES

- [1] "Noise Generators," *ValueTronics International*. [Online]. Available: <https://www.valuetronics.com/signal-generators/noise>. [Accessed: 17-Feb-2022].
- [2] V. Prodanov, "EE452_Description_W2022_v2", California Polytechnic University at San Luis Obispo, Rev. Jan. 2022.
- [3] Texas Instruments, "MF10-N Universal Monolithic Dual Switched Capacitor Filter", MF10 datasheet, June 1999 [revised April 2013]

Category	Results	Goal
Passive voice	9 (5%)	Less than 10%
Wordiness	5 (2%)	Less than 2%
Sentences	0 (0%)	Less than 2%
Transitions	34 (19%)	More than 10%
Academic Style	5 (0%)	Less than 1%
Grammar	0	0 errors
Nominalizations	97 (3%)	Less than 6%
Eggcorns	0	0 errors